Zooplankton biomass and abundance in the Coastal Transition Zone off Northwest Africa

Juan Carlos Garijo López

Instituto de Oceanografía y Cambio Global, Universidad de Las Palmas de Gran Canaria, Campus de Tafira. 35017 Gran Canaria, Spain. E-mail: jgarijo@becarios.ulpgc.es

Director Académico: Santiago Hernández León

Tesina de Máster en Oceanografía

Universidad de Las Palmas de Gran Canaria

Diciembre 2011

Zooplankton biomass and abundance in the Coastal Transition Zone off Northwest Africa

ABSTRACT

The influence of mesoscale activity on zooplankton biomass, abundance, size-fraction distribution and taxonomical composition was studied along a transect from the coastal waters off the NW African upwelling to the offshore waters of the Canary Islands. The transect crossed an upwelling filament and an island-induced anticyclonic eddy southward off Gran Canaria. A second transect was carried out in order to study the three-dimensional structure of the eddy. Samples were scanned and analyzed using digital image processing (ZooImage). Our results confirm the influence of the mesoscale structures on the zooplankton distribution. The upwelling filament enriched the anticyclonic eddy located offshore, promoting an increase in biomass and abundance of zooplankton. Due to the clockwise rotation of the eddy, phyto-and zooplankton concentrated at its edges and core, both experiencing a decrease as the eddy rotated. Medium size organisms were dominant while copepods were the most abundant group, with predominance of small and intermediate size-fractions. The largest individuals (>1000 µm) were observed near the upwelling region and the filament, while small organisms (200-500 µm) were dominant in oceanic waters. Strikingly, medium size zooplankton (mainly copepods in the 500-1000 µm size fraction) was observed near the core of the anticyclonic eddy, suggesting size selectivity inside this mesoscale structure.

1. INTRODUCTION

The Canary Current System (CCS) is one of the major eastern boundary upwelling regions of the world. Like all these systems, and mainly during the upwelling season, is characterized by the generation of a transition zone between the cool, nutrient-rich upwelled waters near the African coast and the warmer and oligotrophic off-shore waters. This Coastal Transition Zone (CTZ) off NW Africa has an intense mesoscale oceanographic activity, promoting the formation of long and narrow filaments flowing off-shore and exporting nutrients and biomass to poorer areas (Barton et al., 1998). Thus, the colder and lower salinity waters from the upwelling region (Barton et al., 1998; Navarro-Pérez and Barton, 1998; García-Muñoz, 2004) are displaced with their chlorophyll richness (Hernández-Guerra et al., 1993; Arístegui et al., 1997; Basterretxea and Arístegui, 2000), mesozooplankton and neritic fish larvae (Rodríguez et al., 1999; Hernández-León et al., 2002a; Rodríguez et al., 2004) to open ocean waters.

The rough orography of the Canary Islands and the particular shape of the Archipelago represent a natural barrier for the regular flow of the Canary Current and the Trade Winds, resulting on the increasing of the mesoscale activity and the formation of cyclonic and anticyclonic eddies. They are formed as the current flows through the islands edges and follow southward with the general flow of the Canary Current. The upwelling filaments, mainly generated by the presence of geographic obstacles, such as a cape, normally interact with eddies flowing downstream the island (Arístegui et al., 1994; Barton et al., 1998, 2004; Sangrá et al., 2005). The filaments are normally trapped into the eddies, giving place to their enrichment and leading to a combined displacement of both structures southward, influencing the plankton transport and distribution in the region (Hernández-León, 1988a, 1991; Arístegui et al., 1997; Rodríguez et al., 2001; Arístegui et al., 2004).

Island-induced eddies can easily reach 100-200 km of magnitude, interacting with the surrounding waters and exchanging with them not only water properties but organic matter as well (Arístegui et al., 2004; Barton et al., 2004; Sangrá et al., 2005). Since they introduce water masses in areas where the conditions are rather different, not only in physical but also in biological patterns, such as community composition, biomass or abundance, they may considerably alter the trophic relationships of the

communities (Hernández-León, 1991; Arístegui et al., 1997; Rodríguez et al., 2001; Hernández-León et al., 2002a; Arístegui et al., 2004). Cyclonic eddies promote isotherm elevation, giving rise to localized upwellings and the increasing of the primary production in their cores (Arístegui et al., 1997). Zooplankton biomass accumulates around them, showing high feeding and growth rates (Hernández-León et al., 2001b). In contrast, anticyclonic eddies trap surrounding surface waters, carrying phyto-and bacterioplankton as well as zooplankton into deeper layers, accumulating them in their cores (Hernández-León et al., 2001b). In any case, the overall significance and mechanisms of the upwelling filaments in the export of plankton to oligotrophic waters is still poorly known. Similarly, the capacity of eddies to transport organic matter still remains uncertain, since it depends on the interactions between these structures and the filaments, and the strength and seasonality of the upwelling events (Álvarez-Salgado et al., 2001).

Zooplankton plays a key role in the biogeochemical cycles in the ocean. It occupies a central position in the pelagic trophic chain, connecting the microbial food web with the larger organisms (Hernández-León et al., 2007). Mesozooplankton feed on phytoplankton and microzooplankton, but they are widely ingested by small pelagic fish as well as numerous fish larvae and micronektonic crustaceans which carry out diel vertical migrations (Putzeys and Hernández-León, 2005; Hernández-León et al, 2010). The latter organisms, after ingesting the zooplankton at the shallower layers migrate to deeper layers in order to avoid predators (Moore, 1950). In this way, zooplankton recycles, redistributes and exports material and energy, not only at the different levels of the trophic web, but also horizontally and vertically in the water column (Banse, 1995). It plays an important role in the active carbon flux from the surface to the mesopelagic zone, being a significant component of the biological pump in the ocean, fundamental to understand the carbon cycle at a global scale (Hernández-León et al., 2010).

Due to their central position in the trophic web, zooplankton plays a key role on the control of communities located in the upper and lower levels. Thus, zooplankton biomass, abundance, taxonomical composition and distribution are of paramount importance to know the functioning of the trophic web in the ocean.

The determination of zooplankton biomass by standard methods implies the destruction of samples. In order to avoid it, and to reduce the time to obtain valid

results, some alternative methods based on image processing have gained prominent role in the last years (Hernández-León and Montero, 2006).

Ortner et al. (1979) and Edgerton (1981) were the first to capture the silhouette of a living planktonic organism trough a conventional camera and an electronic flash. Subsequently, video cameras were used to extract the silhouette of preserved organisms in order to classify them into taxonomical groups (Jeffries et al, 1984). Moreover, some systems based on microscopic images were used to study the size distribution in zooplankton samples (Rolke and Lenz, 1984). Gorsky et al. (1989) developed a method to determine the body area and size in copepods, but only some preliminary results such as the treatment of samples and the analysis process were presented. A more recent method uses a scanner in order to digitalize zooplankton preserved samples (*Zooscan*). The images obtained allow sizing and identification of organisms in an automated way (Grosjean et al., 2004). The software provides in a few minutes valuable results such as individual body length, size spectrum of organisms, abundance or taxonomical composition of the samples (Gorsky and Grosjean, 2003).

In this study, zooplankton samples obtained in two transects of the CTZ off NW Africa were analyzed using *ZooImage 1*. The aim of this work was double since one objective was to test the efficiency of this system as a tool to classify the organisms into the main taxa and estimate zooplankton biomass, abundance and size-fraction distribution. The second one focused on the determination of the biological effect of filaments and eddies on mesozooplankton communities in the CTZ off NW Africa.

2. MATERIAL AND METHODS

During the CONAFRICA cruise (22 March-7 April 2006) on board the R/V "Hespérides", two transects of 12 and 5 stations respectively were sampled from the coastal upwelling waters of the NW Africa to the offshore waters of the CTZ region (Fig. 1). Transect 1 was carried out to study the biomass, abundance, taxonomical composition, and distribution of zooplankton along an upwelling filament flowing to the oligotrophic region, as well as an anticyclonic eddy south off Gran Canaria. The second transect was carried out to better picture the eddy three-dimensional structure. Temperature, salinity and fluorescence were recorded down to 200 m depth using a

SeaBird 911 plus CTD system, mounted on a General Oceanics rosette sampler, equipped with twenty-four 12 l Niskin bottles. Phytoplankton chlorophyll was derived from depth profiles of *in situ* fluorescence calibrated with samples collected at 8-10 depths within the upper 200 m of the water column. In order to detect upwelling filaments occurring in the region, chlorophyll *a* images derived from Seaviewing Wide Field-of-view Sensor (SeaWiFS) on the Sea Star satellite were processed (Fig. 2). Zooplankton samples were collected at 10 different depths from the surface to 200 m depth using a Longhurst-Hardy Plankton Recorder (LHPR) with a 200 µm mesh. Samples were immediately stored in 4% buffered formalin.

In the laboratory, larval and fish eggs were removed for further analysis. Thereafter, every sample was fractionated using a 1000 µm mesh net in order to simplify the image processing. These subsamples were fractionated using a *Folsom Plankton Splitter* and spilled into 90 x 130 mm polystyrene plates. Overcrowded plates would cause system conflicts and mistaken results because the software would recognize several superimposed organisms as a unique individual, giving the idea that the organisms were bigger. Once we had the adequate number of organisms per plate, the scanning process was carried out using an *Epson Perfection 4990 PHOTO* scanner at a resolution of 1200 dpi. The software used in this study, *ZooImage 1 version 1.2-1*, required a *Tiff* format to analyze the images whose sizes ranged around 42-43 Mb each one. This is a free-license software that may be actually downloaded from its own web page.

After all the subsamples were digitally stored, the images were processed in order to obtain the body length, area or shape of the organisms. Those parameters were basic for the biomass determination, size spectrum recognition or abundance estimations. Depending on the number of organisms per sample, the processing time was variable, ranging from 2-3 minutes for the least abundant to 8-10 for those where the number of analyzed particles was greater than 1500-2000, coinciding with the smaller organisms fractions.

The software proportioned one different picture for every single particle present on the samples. This was crucial in the taxonomical classification of the organisms. Using these new created images, a *training set* was manually performed in order to use the *ZooImage 1* to classify the organisms into taxons. This set was used afterwards by the machine as an example to establish division patterns between the different groups

during the sample processing. In our case, in order to minimize the error, a set of near 2000 images were classified into 5 taxonomic groups: Chaetognatha, Euphausiid-like, Copepoda, Gelatinous zooplankton and Other Mesozooplankton. Normally, a regular *training set* requires a much more lower number of images. However, the huge diversity found in this area of the Canary Current forced to raise these numbers, achieving a global error of only 6.9% in the taxonomical classification

The Chaetognatha and Copepoda were just integrated by organisms belonging to these taxons; in contrast, the others were forced to embrace some other categories to reduce the global error. Thus, Euphausiid-like group included mysids, decapods larvae (brachyura) and euphausiids. Likewise, the siphonophore and thaliacean individuals were integrated into the Gelatinous category. Similarly, the Other Mesozooplankton group was composed by all the organisms that were not abundant enough to form a taxonomic group by themselves, such as amphipoda, cladocera, appendicularia, ostracoda, polychaeta, isopoda, pteropoda, other larvae or some unidentified organisms. In all these cases, the scarce individuals found on the samples determined their inclusion together. The inorganic particles were included in an extra group in order to discard them during the estimation of biomass and abundance; that was the case of marine snow, bubbles or fibers.

Prior to biomass estimation and once the organisms were measured and classified into the defined categories, it was necessary to establish some biomass conversion factors in order to relate the size of the organisms with their dry mass. *ZooImage 1 version 1.2-1* established the relationship:

$$Y = (P1\ x + P2)^{P3}$$

where Y was the biomass (mg of dry weight), x was the parameter automatically measured during the image analysis (by defect ECD or Equivalent Circular Diameter) and P1, P2, P3 were the allometric parameters, required to estimate the biomass. However, in this study we used the relationships developed by Lehette and Hernández-León (2009, see Table 1), which supposed an improvement of those obtained by Hernández-León and Montero (2006). The area of the organisms was obtained from the ECD provided by the software from every individual. In order to compare with previous studies in the area, we also studied three different size groups: 200-500 µm, 500-1000 µm and >1000 µm.

3. RESULTS

Despite some sporadic downwelling-favourable winds occurred before the CONAFRICA cruise at the end of February, the sampling was carried out during an upwelling event. That was corroborated by the time-series of wind speed and direction averaged over the area of study (Benítez-Barrios et al., 2011). Besides, the salinity and temperature in transect 1 (Fig. 3a) clearly showed an area of colder and less salty water at stations located over the African shelf. The presence of a filament-eddy system was observed from the satellite-derived chlorophyll *a* images (Fig. 2), where it was clear the displacement toward the ocean of the chlorophyll-rich filament from the upwelled coastal waters. Filament-eddy associations have been previously well described for the same region (Barton et al., 2004). The existence of sharp fronts in temperature and salinity distribution along transect 1 reinforced this idea. Moreover, these fronts seemed to indicate that section 1 crossed the filament from stations 36 to 51 (Fig 3a). This filament entered an anticyclonic eddy (Fig. 2) of approximately 70-85 km diameter generated southeast off Gran Canaria, as indicated by the sharp gradients of salinity and temperature at the interfaces eddy-filament (St. 64) and eddy-open ocean (St. 74). The eddy entrained warmer and saltier water and it seemed to be centered at station 70 (Baltar et al., 2009), although the salinity and temperature distribution along transect 2 indicated that the real center was rather displaced some kilometers toward the north, around station 69 (Fig. 3b). The filament interacted with the anticyclonic eddy as observed by the chlorophyll enrichment of this latter structure (Fig. 3a). In transect 1, chlorophyll *a* mainly accumulated at the eastern edge of the eddy (St. 64), with comparative levels to those observed in the upwelling area (Sts. 4-11) and the filament (Sts. 43-51) (Fig. 3a). On the other hand, in transect 2 the chlorophyll *a* mainly accumulated at the northern edge of the eddy (Sts. 67-68) and at the station 70. Chlorophyll *a* was also observed at deeper layers, near its core (Fig. 3b).

As expected, zooplankton biomass was highest in stations located on the African shelf (Sts. 4 to 20), coinciding with the true upwelled waters (Fig. 4a). Thus, peak values of about 20 mg of dry weight · m^{-3} were observed in the upper 80 m of the water column. Maximum values of 10-12 mg of dry weight · m^{-3} were related to the filament and the anticyclonic eddy (Fig. 4 a,b). In fact, mean values of biomass were similar in both structures (Table 2). Differencees between the average biomass values

in both transects were statistically significant (ANOVA, $p<0.05$), being higher in transect 1 than in transect 2 (Table 2), even though the first included the enormous productivity of the upwelling waters. The highest values of biomass in the eddy were mostly observed on the eastern and southern boundaries (Sts. 57 and 70-71, respectively) and markedly at the core, at stations 51 to 70 in transect 1 and 68 to 71 in section 2 (Fig. 4a,b). The peak of biomass in the core was found deeper than the maximum of chlorophyll (Fig. 3b).

Copepod biomass was 65-80% of total biomass, while in terms of abundance the averaged value was about 85% (Table 3). Discerning between areas, copepods were more abundant in the upwelling front (St. 20), the filament (Sts. 36-43) and the center and the northern edge of the eddy (St. 70 and 67-68, respectively) (Fig. 4a,b), being their abundance similar in all these areas (85-100%). The highest biomass of copepods was found in the first 100 meters of the water column in the upwelling zone, at stations 4 and 11, both located on the African shelf (Table 2). Likewise, elevated values were associated to the upper 50 m of the filament (Sts. 43-51) (Fig. 4a), where the biomass of copepods represented on average more than 75% of the total (Table 2). Comparative values were also associated with the core and the eastern and southern edges of the anticyclonic eddy, as observed in transect 1 (Sts. 57 to 70), as well as in the section 2 (Sts. 68 to 71) (Fig. 4a,b).

Chaetognatha was, in general, the second most abundant taxa in both sections, increasing its abundance toward the ocean (Table 3), although decreasing inside the eddy. (Fig. 5a). The Other Mesozooplankton group reached a similar abundance to chaetognaths in transect 2, (Fig. 5b) whereas the low abundance of gelatinous slightly increased toward the ocean, with higher values associated to the boundaries of the eddy (Sts. 57 and 74) (Fig. 5a). The abundance of euphausiid-like organisms clearly decreased to the ocean, observing higher biomass in the upwelling zone (Sts. 4 and 11) and the filament (Sts. 27 to 43), as well as in the southern edge of the eddy (Sts. 70 to 72) (Fig. 5 a,b), coinciding with samples obtained during night.

The size fractioned abundance given by *ZooImage 1* showed the highest values in the 500-1000 µm fraction, which represented about 61% of the total abundance (Table 4); the 200-500 µm and >1000 µm fractions accounted for 28% and 10%, respectively (Fig. 6a,b). The smallest organisms showed low abundances in the upwelling waters (Fig. 6a), being this area dominated by the intermediate size fraction

(Table 4), being these two fractions dominant in the filament (Sts. 36 to 51). The maximum abundance of the small fraction, ranging from 30 to 40%, was related to the upper 25 m along the eddy (Sts. 64 to 76) as well as to its northern and southern boundaries below some 50 m depth (Sts. 67 and 71, respectively) (Fig. 6 a,b). Outside the upwelling zone, the intermediate fraction showed its highest abundance along the eddy (Table 4), with slightly higher values associated to the boundaries (Sts. 64 and 74), mainly to the east (Fig. 6 a,b). On the other hand, the highest abundance of the larger fraction was related to the upwelling. Besides, comparative values were observed at some stations along the filament (Fig. 6a). The distribution of the different size-fractions of copepods in terms of abundance differed from the one observed for the total groups, since the abundance of the medium size and small copepods was almost identical (Table 4). Intermediate size copepods were mainly associated to the eddy, especially with the center (St. 70) and the very upper layers of this mesoscale structure (Sts. 67 to 71) (Fig. 7 a,b). On the other hand, the smallest copepods were mainly distributed at the boundaries of the eddy and more acutely on the west and north (Sts. 74-76 and 68, respectively) with an abundance greater than 45% at these stations (Fig. 7 a,b). Larger copepods were more abundant in the filament (Sts. 36-43) and the upwelling (Sts. 4 to 20) as well as in the upper layers of the filament-eddy edge (St. 64) (Fig. 7 a); although in lower abundance, some large individuals were observed in the core of the eddy (Sts. 69 to 71) (Fig. 7b).

4. DISCUSSION

ZooImage 1 proved to be a helpful tool for this kind of studies, since it supposed a considerably time-saving procedure in comparison with the traditional methodology. The error achieved when classifying the organisms into taxons was lower in comparison with similar studies, such as 20-30% (Benfield et al., 2007) or 12.5% (Bell et al., 2008), although in this latter study the authors used a more complex set of data.

Our results show that the observed mesoscale structures clearly influenced the patterns of distribution, abundance and composition of zooplankton in the CTZ, with a close relationship between the biomass and the physical signatures. The filament extending off-shore from the upwelling waters exported chlorophyll *a* and zooplankton

to the oligotrophic region, giving rise to an increase in biomass and abundance of zooplankton. This is in agreement to the results observed by Baltar et al. (2009) for nano- and picoplankton, Mackas et al. (1991) and Hernández-León et al. (2001b, 2002a, 2007) for mesozooplankton and Rodriguez et al. (1999), Brochier et al. (2008), Bécognée et al. (2009) and Brochier et al. (2011) for ichtyoplankton.

Mean values of zooplankton biomass along the transects (Table 2) were higher than those obtained by Rodriguez et al. (2001) in the same waters, who observed an average biomass of 4.5±2.7 mg of dry weight · m^{-3}. This difference should be related to the seasonality (March-April *vs.* October-November) and the high mesoscale variability of the CTZ. As expected, zooplankton biomass was higher in the productive waters of the upwelling and remained relatively high at the upwelling front (Fig. 3a), probably influenced by the filaments extending off-shore. The 500-1000 µm size-fraction was the most abundant in the area of study (Table 4), showing a slight decrease along the filament and increasing within the anticyclonic eddy, where its abundance was comparative to the upwelling (Fig. 6a,b). The largest individuals (>1000 µm) were observed near the upwelling region and the filament and experienced a decrease toward the ocean, whilst small organism (200-500 µm) were dominant in oceanic waters (Fig. 6a). This distribution followed the general pattern in the region as observed by Hernández-León et al. (2002a), who suggested predation as the main mechanism in the control on large individuals.

As expected, higher values of chlorophyll *a* were observed at the rich waters of the upwelling (Fig. 3a), with distribution following the physical signature as occurred with zooplankton. The meandering of the filament (Fig. 2) was observed as a patchy distribution in those areas where transect 1 crossed the structure, mainly in the upper layers (Fig. 3a). The transport of chlorophyll by upwelling filaments is in agreement to Hernández-Guerra et al. (1993), Basterretxea (1994), Arístegui et al. (1997) and Basterretxea and Arístegui (2000). This load of chlorophyll enriched the anticyclonic eddy, giving rise to an increase in the biomass and abundance of zooplankton within the structure, similar to the findings by Hernández-León et al. (2002a, 2007). Moreover, Hernández-León et al. (2001b) determined that eddies can promote the accumulation of biomass southward of the islands as a result of their inward motion while being formed.

Due to the clockwise rotation of the eddy, the organisms mostly concentrated on the boundaries and the core, as observed by Hernández León et al. (2001b, 2007) for

mesozooplankton and Rodríguez et al., (2004) for ichtyoplankton. This is also consistent with other studies performed with copepods (Postel, 1982; Richardson and Verheye, 1999; Hernández-León et al., 2002a; Yebra, 2002; Yebra et al. 2004). In the present study, higher biomass was mostly associated to the eastern and southern boundaries of the eddy and markedly to the core, with similar values to those of the filament. As the eddy rotated the biomass decreased (Fig. 4a,b) as well as chlorophyll (Fig. 3a,b), suggesting that grazing controlled primary production. The fact that larger copepods (>1000 μm) turned more scarce on the western and northern boundaries of the eddy (Fig. 7a,b) suggests size selectivity.

The distribution of zooplankton biomass and size fractions abundance did not always match the physical structure observed. The boundaries of the eddy, where the organisms mostly concentrated, seem to be displaced from the position indicated by the physical signature, as also observed by Hernández-León et al. (2001b). In this sense, newly formed eddies are ageostrophic and their vertical and horizontal structure changes during their development, generally having elliptical shapes (Arístegui et al., 1994). The vertical structure of eddies normally changes in the upper layers, where the zooplankton distributes, introducing important variability. Besides, some models developed to study the disturbance in the Canary Current passing through Gran Canaria showed the formation of asymmetrical cyclonic and anticyclonic eddies (Sangrá, 1995; Arístegui et al., 1997). In our case, the center of the eddy in the shallower layers did not vertically coincide with the core deeper, having some asymmetry (Fig. 3b). This fact would better explain the higher abundance of phyto-and zooplankton on the real boundaries of the eddy, as it would rather have an elliptical shape with its east-west axis more elongated. This may be also appreciated when observing the high biomass accumulated below 150 m in the core of the eddy, since the organisms in transect 1 appeared to be distributed along a larger area than in the section 2 (Fig. 4a,b). This vertical variability could explain why the biomass in the core did not coincide with the maximum of chlorophyll (Fig. 3b).

Copepods were the most numerous group (Table 3), considering their abundance into the range observed by Hernández-León (1988b) and Hernández-León et al. (1998, 2002a, 2007) in the same waters. Hernández-León et al. (2002a) also observed predominance of middle-size and large copepods. However, in our case intermediate and small copepods were dominant, whereas the largest individuals decreased toward

the ocean (Fig. 7a,b). Unlike the observed decrease in the abundance of copepods and chaetognaths to the ocean (Hernández-León et al., 2002a), in our study their values remained high along the transects or even increased in chaetognaths (Table 3). Although the eddy was dominated by copepods, chaetognaths represented more than 10% of the total biomass along the structure (Fig. 5a,b). Furthermore, their abundance increased on its boundaries as observed by Hernández-León et al. (2007) in a cyclonic eddy in the same waters. The biomass of euphausiids decreased toward the ocean, although the variability in their abundance seemed to be more influenced by the migratory nature of this species (Hernández-León et al., 2001a; Yebra et al., 2005), since their biomass did not follow a clear coastal-open ocean pattern (Fig. 5a,b).

Small copepods were more numerous in the surface layers of the anticyclonic eddy, with the lowest values in the core (Fig. 7a,b), as observed by Yebra et al. (2004). By opposite, the larger ones although less abundant were associated to the boundaries and the core of the structure (Fig. 7b), where a maximum of chlorophyll was detected (Fig. 3b). Hernández-León et al. (2001b) suggested a top-down effect of the larger organisms upon the smaller ones to explain these inverse values. Moreover, they suggested, as well as Hernández-León et al. (2007), that the swimming capabilities of the large and intermediate-size copepods promote their accumulation by the edges and the core of anticyclonic eddies, where an increment in the ambient food exists, as phytoplankton is advected to their boundaries and pushed to deeper layers. This could also explain the higher abundance of the 500-1000 μm copepods by the edges and the core of the eddy (Fig. 7a,b).

The high biomass observed in samples obtained during night (Fig. 4a,b) might be related to migrating zooplankton, as they were associated to an increase in the biomass of migratory species, such as euphausiids (Fig. 5a,b). Biomass increases during night samplings have been well documented in the study area and they are not due to merely the possible increase of effectiveness of the hauls by night (Hernández-León et al., 2001a; Yebra et al., 2005), verifying the relevance of migrants in the carbon fluxes (Putzeys and Hernández-León, 2005; Hernández-León et al., 2010). In addition, Yebra et al. (2005) suggested that the elevated concentration of food, both phytoplankton and zooplankton occurring in anticyclonic eddies, enhances vertical migration of these predators from the deep scattering layers (DSL). Besides, Hernández-León (1998) and Hernández-León et al. (2001a, 2002b, 2007) suggested that these organisms may

control epizooplankton in these waters. Unfortunately, our samplings along the eddy mostly coincided with the illuminated period; the analysis of the acoustic data (in prep.) could lead to clearer conclusions.

In summary, the results obtained confirm the influence of the mesoscale structures on the zooplankton distribution in the CTZ off NW Africa. The upwelling filament enriched the anticyclonic eddy, giving rise to an increase of biomass and abundance of zooplankton offshore. The organisms were more abundant at the edges and core of the eddy, decreasing their biomass as it rotated. Zooplankton distributed following a pattern of size, with the largest individuals near the upwelling region and the filament, while smaller ones were dominant offshore. Intermediate size organisms were the most abundant fraction and copepods were the most numerous group, with a similar abundance of the small and intermediate size-fractions. The observed size distribution inside the eddy suggested size selectivity within this structure. Further studies are needed to clarify the overall significance and mechanisms of the upwelling filaments in the export of plankton to oligotrophic waters and the capacity of eddies to transport organic matter.

REFERENCES

Álvarez-Salgado X.A., Doval M.D., Borges A.V., Joint I., Frankignoulle M., Woodward E.M.S., Figueiras F.G. (2001) Off-shelf fluxes of labile materials by an upwelling filament in the nw iberian upwelling system. Progress in Oceanography 51:321-337.

Arístegui J., Sangrá P., Hernández-León S., Cantón M., Hernández-Guerra A., Kerling J.L. (1994) Island-induced eddies in the Canary islands. Deep-Sea Research Part I 41:1509-1525.

Arístegui J., Tett P., Hernández-Guerra A., Basterretxea G., Montero M.F., Wild K., Sangrá P., Hernández-León S., Cantón M., García-Braun J.A., Pacheco M., Barton E.D. (1997) The influence of island-generated eddies on chlorophyll distribution: A study of mesoscale variation around Gran Canaria. Deep-Sea Research Part I: Oceanographic Research Papers 44:71-96.

Arístegui J., Álvarez-Salgado X. A., Barton E. D., Figueiras F. G., Hernández-León S., Roy C., Santos A. M. P. (2004) Oceanography and fisheries of the Canary Current/Iberian region of the Eastern North Atlantic. In: Robinson A. R., Brink K. H. (Eds.), The Sea, vol. 14. Harvard University Press, Cambridge, MA.

Baltar F., Arístegui J., Montero M.F., Espino M., Gasol J.M., Herndl G.J. (2009) Mesoscale variability modulates seasonal changes in the trophic structure of nano- and picoplankton communities across the NW Africa-Canary Islands transition zone. Progress in Oceanography 83:180-188.

Banse K. (1995) Zooplankton: pivotal role in the control of ocean production. ICES Journal of Marine Science 52:265–277.

Barton E.D., Aristegui J., Tett P., Canton M., García-Braun J., Hernández-León S., Nykjaer L., Almeida C., Almunia J., Ballesteros S., Basterretxea G., Escanez J., García-Weill L., Hernández-Guerra A., López-Laatzen F., Molina R., Montero M.F., Navarro-Peréz E., Rodríguez J.M., Van Lenning K., Vélez H., Wild K. (1998) The transition zone of the Canary Current upwelling region. Progress in Oceanography 41:455-504.

Barton E.D., Arístegui J., Tett P., Navarro-Pérez E. (2004) Variability in the Canary Islands area of filament-eddy exchanges. Progress in Oceanography 62:71-94.

Basterretxea G. (1994) Influencia de las estructuras oceanográficas mesoescalares sobre la producción primaria en la región canaria. Ph. D. Thesis, University of Las Palmas de Gran Canaria, Spain.

Basterretxea G., Arístegui J. (2000) Mesoscale variability in phytoplankton biomass distribution and photosynthetic parameters in the canary-NW African coastal transition zone. Marine Ecology Progress Series 197:27-40.

Bécognée P., Moyano M., Almeida C., Rodríguez J.M., Fraile-Nuez E., Hernández-Guerra A., Hernández-León S. (2009) Mesoscale distribution of clupeoid larvae in an upwelling filament trapped by a quasi-permanent cyclonic eddy off Northwest Africa. Deep-Sea Research Part I: Oceanographic Research Papers 56:330-343.

Bell J.L., Hopcroft R.R. (2008) Assessment of ZooImage as a tool for the classification of zooplankton. Journal of Plankton Research 30:1351-1367.

Benfield et al. (2007) RAPID: Research on Automated Plankton Identification. Oceanography, 20, 172–187.

Benítez-Barrios V.M., Pelegrí J.L., Hernández-Guerra A., Lwiza K.M.M., Gomis D., Vélez-Belchí P., Hernández-León S. (2011) Three-dimensional circulation in the NW Africa coastal transition zone. Progress in Oceanography.

Brochier T., Ramzi A., Lett C., Machu E., Berraho A., Fréon P., Hernández-León S. (2008) Modelling sardine and anchovy ichthyoplankton transport in the Canary current system. Journal of Plankton Research 30:1133-1146.

Brochier T., Mason E., Moyano M., Berraho A., Colas F., Sangrà P., Hernández-León S., Ettahiri O., Lett C. (2011) Ichthyoplankton transport from the African coast to the Canary Islands. Journal of Marine Systems 87:109-122.

Edgerton H. E. (1981) Electronic flash sources and films for plankton photography. Journal of Biology Photogr. 49:25–26.

Jeffries H. P. (1984) Automated sizing, counting and identification of zooplankton by pattern recognition. Marine Biology 78:329–334.

García-Muñoz M., Arístegui J., Montero M.F., Barton E.D. (2004) Distribution and transport of organic matter along a filament-eddy system in the Canaries - NW Africa coastal transition zone region. Progress in Oceanography 62:115-129.

Gorsky G., Guibert P., Valenta E. (1989) The autonomous image analyzer: enumeration, measurement and identification of marine phytoplankton. Marine Ecology Progress Ser. 58:133–142.

Gorsky G., Grosjean P. (2003) Qualitative and quantitative assessment of zooplankton samples. GLOBEC Int. Newsletter 9:5–6.

Grosjean P., Picheral M., Warembourg C., Gorsky G. (2004) Enumeration, measurement and identification of net zooplankton samples using the Zooscan digital imaging system. Ices Journal of Marine Science 61:518–525.

Hernandez-Guerra A., Aristegui J., Canton M., Nykjaer L. (1993) Phyoplankton pigment patterns in the Canary Islands area as determined using coastal zone colour scanner data. International Journal of Remote Sensing 14:1431-1437.

Hernández-León S., Linas O., Braun J. G. (1984) Nota sobre la variación de la biomasa del mesozooplancton en aguas de Canarias. Investigaciones Pesqueras 48(3):495-508.

Hernández-León S. (1988a) Gradients of mesozooplankton biomass and ETS activity in the wind-shear area as evidence of an island mass efect in the Canary Island waters. Journal of Plankton Research 10(6), 1141-1154.

Hernández-León S. (1988b) Algunas observaciones sobre la abundancia y estructura del mesozooplancton en aguas del Archipiélago Canario. Boletín Instituto Español de Oceanografía 5(1): 109-118.

Hernández-León S. (1991) Accumulation of mesozooplankton in a wake area as a causative mechanism of the "island-mass effect". Marine Biology 109:141-147.

Hernández-León S. (1998) Annual cycle of epiplanktonic copepods in Canary Island waters. Fisheries Oceanography 7:252-257.

Hernández-León S., Gómez M., Pagazaurtundua M., Portillo-Hahnefeld A., Montero I., Almeida C. (2001a) Vertical distribution of zooplankton in Canary Island waters: Implications for export flux. Deep-Sea Research Part I: Oceanographic Research Papers 48:1071-1092.

Hernández-León S., Almeida C., Gómez M., Torres S., Montero I., Portillo-Hahnefeld A. (2001b) Zooplankton biomass and indices of feeding and metabolism in island-generated eddies around Gran Canaria. Journal of Marine Systems 30:51-66.

Hernández-León S., Almeida C., Yebra L., Arístegui J., Fernández de Puelles M.L., García-Braun J. (2001c) Zooplankton abundance in subtropical waters: Is there a lunar cycle? Scientia Marina 65:59-63.

Hernández-León S., Almeida C., Portillo-Hahnefeld A., Gómez M., Rodríguez J.M., Arístegui J. (2002a) Zooplankton biomass and indices of feeding and metabolism in relation to an upwelling filament off northwest Africa. Journal of Marine Research 60:327-346.

Hernández-León S., Almeida C., Yebra L., Arístegui J. (2002b) Lunar cycle of zooplankton biomass in subtropical waters: Biogeochemical implications. Journal of Plankton Research 24:935-939.

Hernández-León S., Montero I. (2006) Zooplankton biomass estimated from digitalized images in Antarctic waters: A calibration exercise. Journal of Geophysical Research C: Oceans 111.

Hernández-León S., Gómez M., Arístegui J. (2007) Mesozooplankton in the Canary Current System: The coastal-ocean transition zone. Progress in Oceanography 74:397-421.

Hernández-León S., Franchy G., Moyano M., Menéndez I., Schmoker C., Putzeys S. (2010) Carbon sequestration and zooplankton lunar cycles: Could we be missing a major component of the biological pump? Limnology and Oceanography 55:2503-2512.

Lehette P., Hernández-León S. (2009) Zooplankton biomass estimation from digitized images: A comparison between subtropical and Antarctic organisms. Limnology and Oceanography: Methods 7:304-308.

Mackas D. L., Washburn L., Smith S. L. (1991) Zooplankton community pattern associated with a California Current cold filament. Journal of Geophysical Research 96, 14781–14797.

Moore H. B. (1950) The relation between the scattering layer and the euphausiacea. Biology Bulletin 99: 181–212, doi: 10.2307/1538738.

Navarro-Pérez E., Barton E.D. (1998) The physical structure of an upwelling filament off the North-West African coast during august 1993. South African Journal of Marine Science:61-73.

Ortner P. B., Cumming S. R., Aftring R. P., Edgerton H. E. (1979) Silhouette photography of oceanic zooplankton. Nature 277:50–51.

Postel L. (1982) Mesoscale investigations on the space-temporal variability of the zooplankton biomass in upwelling regions off Northwest and Southwest Africa. Rapports et Proces-verbaux des Reunions Conseil International pour l'Exploration de la Mer 180, 274-279.

Putzeys S., Hernández-León S. (2005) A model of zooplankton diel vertical migration off the Canary Islands: Implication for active carbon flux. Journal of Sea Research 53:213-222.

Richardson A.J., Verheye H.M. (1999) Growth rates of copepods in the southern Benguela upwelling system: The interplay between body size and food. Limnology and Oceanography 44:382-392.

Rodríguez J.M., Hernández-León S., Barton E.D. (1999) Mesoscale distribution of fish larvae in relation to an upwelling filament off Northwest Africa. Deep-Sea Research Part I: Oceanographic Research Papers 46:1969-1984.

Rodríguez J.M., Barton E.D., Eve L., Hernández-León S. (2001) Mesozooplankton and ichthyoplankton distribution around gran canaria, an oceanic island in the NE atlantic. Deep-Sea Research Part I: Oceanographic Research Papers 48:2161-2183.

Rodríguez J.M., Barton E.D., Hernández-León S., Arístegui J. (2004) The influence of mesoscale physical processes on the larval fish community in the Canaries CTZ, in summer. Progress in Oceanography 62:171-188.

Rolke M., Lenz J. (1984) Size structure analysis of zooplankton samples by means of an automated image analyzing system. Journal of Plankton Research 6:637–645.

Sangrà P., Pelegrí J.L., Hernández-Guerra A., Arregui I., Martín J.M., Marrero-Díaz A., Martínez A., Ratsimandresy A.W., Rodríguez-Santana A. (2005) Life history of an anticyclonic eddy. Journal of Geophysical Research C: Oceans 110:1-19.

Yebra L. (2002) Study of growth and mortality of zooplankton in the Canary Island waters. Ph. D. Thesis, University of Las Palmas de Gran Canaria, Spain.

Yebra L., Hernández-León S., Almeida C., Bécognée P., Rodríguez J.M. (2004) The effect of upwelling filaments and island-induced eddies on indices of feeding, respiration and growth in copepods. Progress in Oceanography 62:151-169.

Yebra L., Almeida C., Hernández-León S. (2005) Vertical distribution of zooplankton and active flux across an anticyclonic eddy in the Canary Island waters. Deep-Sea Research Part I: Oceanographic Research Papers 52:69-83.

Figure 1. Location of the two transects and the sampling stations.

Figure 2. Stations location on a Sea-viewing Wide-Field-of-view-Sensor (SeaWiFS) chlorophyll image from 7 April 2006. *F* and *A* stand for upwelling filament and anticyclonic eddy, respectively.

Figure 3. Vertical CTD profiles of temperature (ºC), salinity (psu) and chlorophyl *a* ($mg \cdot m^{-3}$) along transects 1 and 2, respectively.

Figure 4. Zooplankton biomass (mg dry $weight \cdot m^{-3}$), copepod biomass (mg dry $weight \cdot m^{-3}$) and copepod abundance (%) distribution along transects 1 and 2, respectively. Red colour indicates night stations.

Figure 5. Averaged values of abundance (%) and biomass (%) for the different zooplankton groups along transects 1 and 2, respectively. Station numbers in red were carried out during the night period.

Figure 6. Distribution of zooplankton abundance (%) for the 200-500 µm, 500-1000 µm and >1000 µm size-fractions along transects 1 and 2, respectively. Station numbers in red were carried out during night.

Figure 7. Distribution of copepod abundance (%) for the 200-500 µm, 500-1000 µm and >1000 µm size-fractions along transects 1 and 2, respectively. Station numbers in red were carried out during night.

Figure 1.

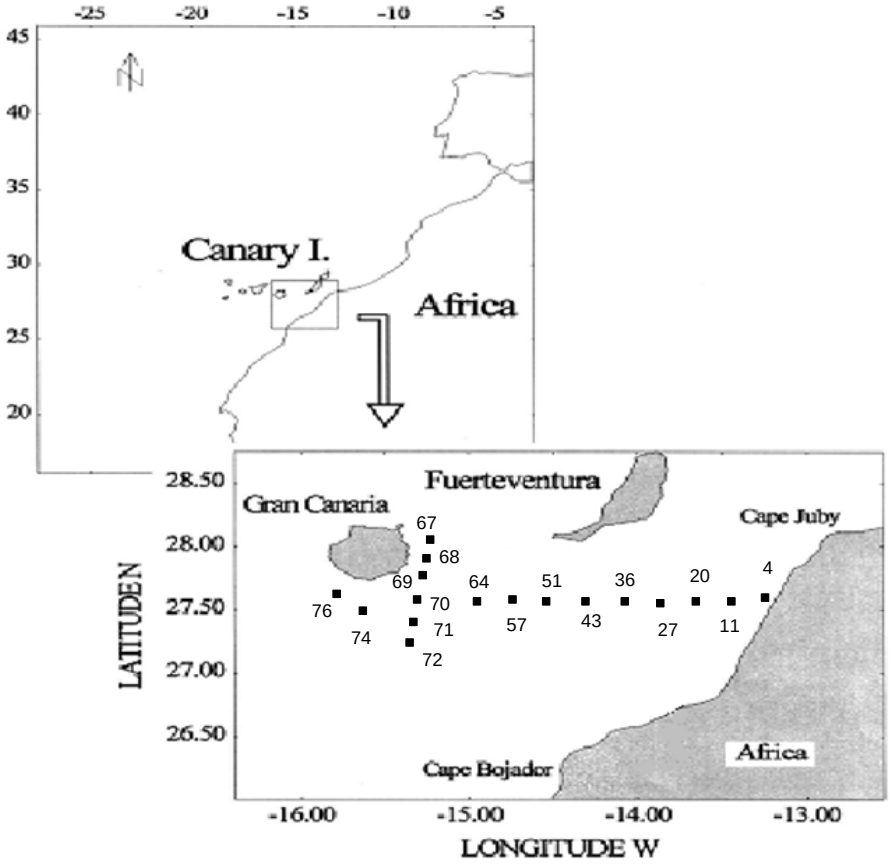
-25
-20
-15
-10
-5
45
40
35
30
25
20
Canary I.
Africa
28.50
28.00
27.50
27.00
26.50
LATITUDE N
Fuerteventura
Gran Canaria
Cape Juby
Cape Bojador
Africa
67
68
69
64
51
36
20
4
76
70
57
43
27
11
74
71
72
-16.00
-15.00
-14.00
-13.00
LONGITUDE W

Figure 2.

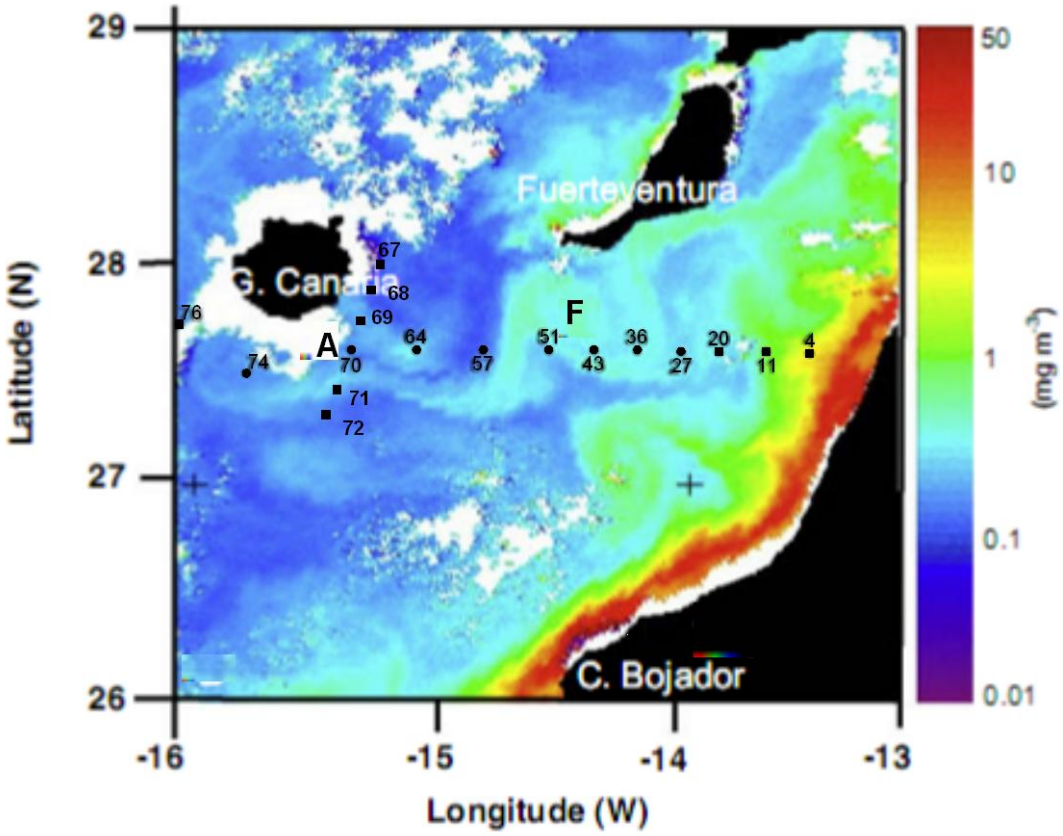
29
28
27
26
-16
-15
-14
-13
Latitude (N)
Longitude (W)
Fuerteventura
C. Bojador
A
F
67
68
69
64
76
74
70
71
72
57
51
43
36
27
20
11
4
50
10
1
0.1
0.01
(mg m-3)

Figure 3.

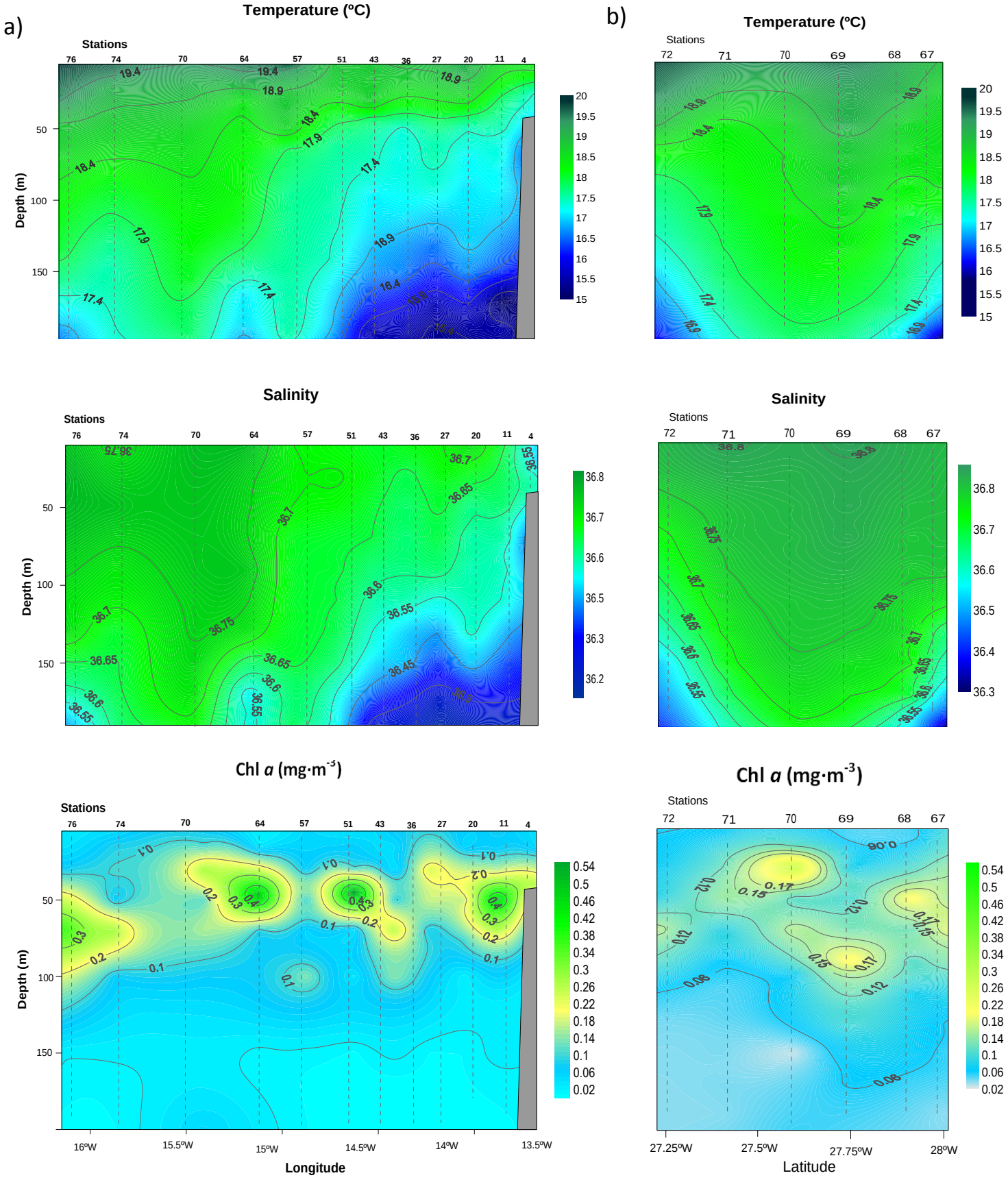
a)
Temperature (ºC)
Stations
Depth (m)
Salinity
Chl a (mg·m-3)
Longitude
b)
Temperature (ºC)
Salinity
Chl a (mg·m-3)
Latitude

Figure 4.

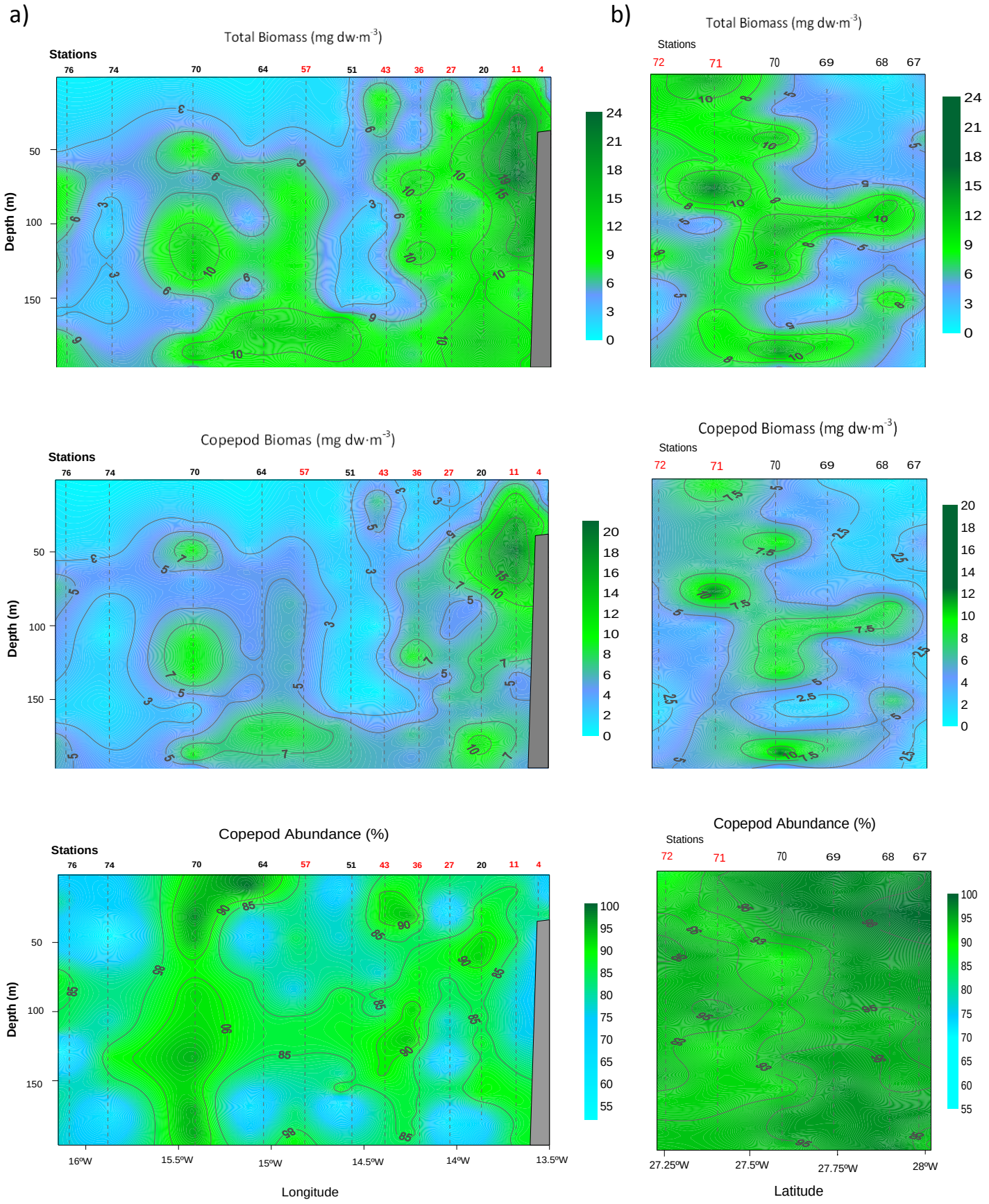
a)
b)
Total Biomass (mg dw·m-3)
Stations
Depth (m)
Copepod Biomas (mg dw·m-3)
Copepod Biomass (mg dw·m-3)
Copepod Abundance (%)
Longitude
Latitude
16ºW
15.5ºW
15ºW
14.5ºW
14ºW
13.5ºW
27.25ºW
27.5ºW
27.75ºW
28ºW

Figure 5.

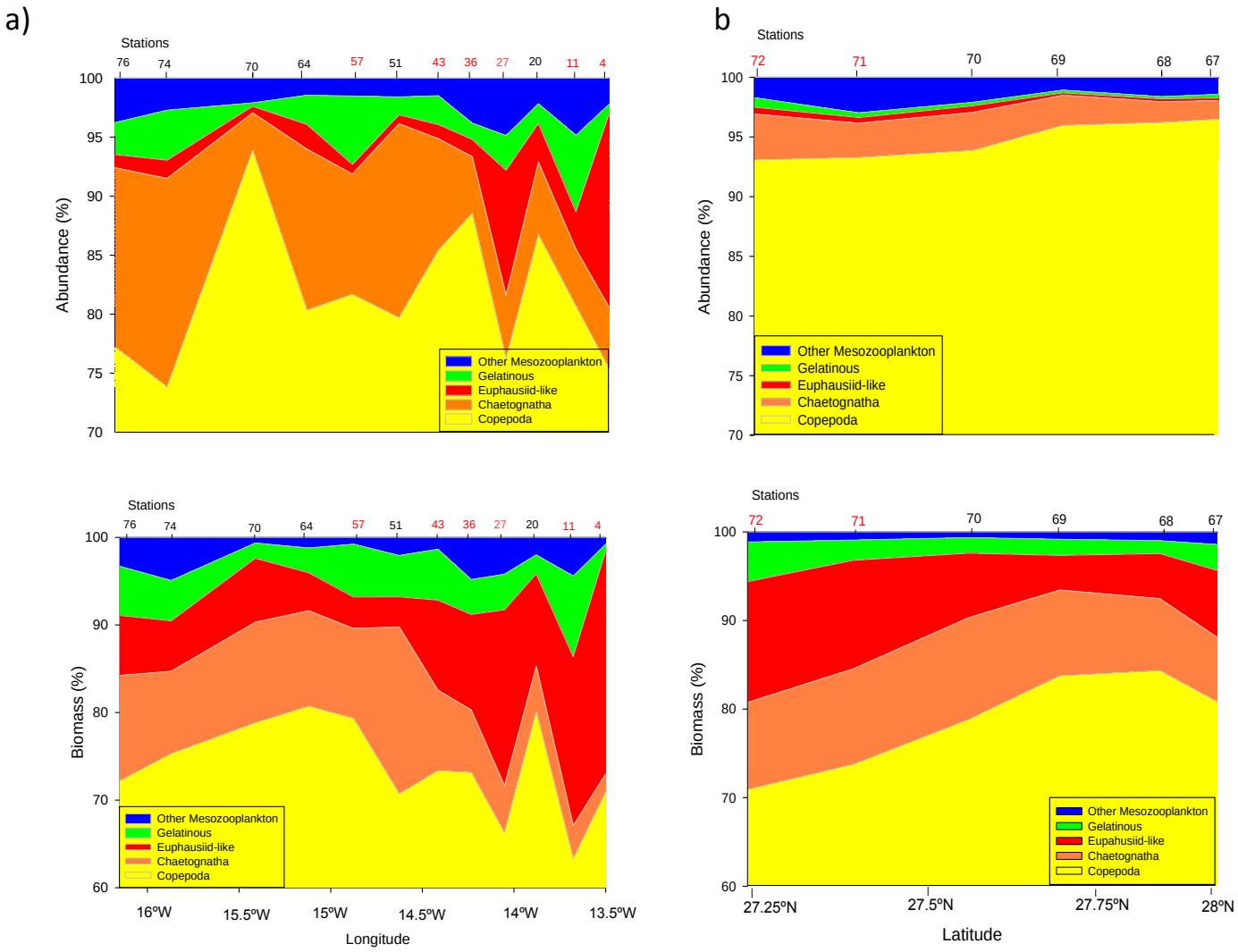
a)
b
Stations
76 74 70 64 57 51 43 36 27 20 11 4
72 71 70 69 68 67
Abundance (%)
Biomass (%)
Other Mesozooplankton
Gelatinous
Euphausiid-like
Eupahusiid-like
Chaetognatha
Copepoda
16ºW 15.5ºW 15ºW 14.5ºW 14ºW 13.5ºW
Longitude
27.25ºN 27.5ºN 27.75ºN 28ºN
Latitude

Figure 6.

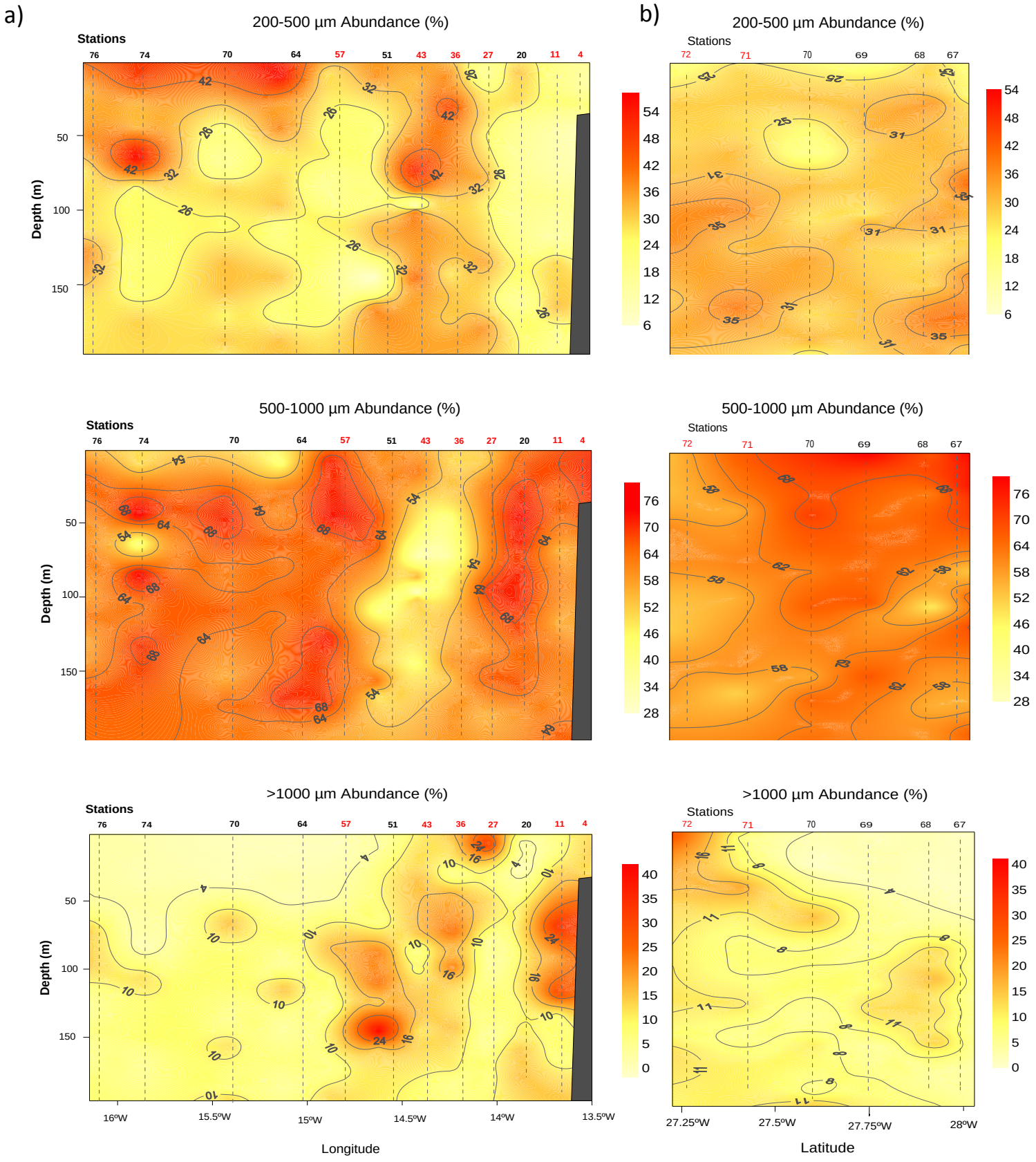
a)
200-500 µm Abundance (%)
Stations
76 74 70 64 57 51 43 36 27 20 11 4
Depth (m)
50
100
150
500-1000 µm Abundance (%)
Stations
76 74 70 64 57 51 43 36 27 20 11 4
Depth (m)
50
100
150
>1000 µm Abundance (%)
Stations
76 74 70 64 57 51 43 36 27 20 11 4
Depth (m)
50
100
150
16ºW
15.5ºW
15ºW
14.5ºW
14ºW
13.5ºW
Longitude
b)
200-500 µm Abundance (%)
Stations
72 71 70 69 68 67
54 48 42 36 30 24 18 12 6
500-1000 µm Abundance (%)
Stations
72 71 70 69 68 67
76 70 64 58 52 46 40 34 28
>1000 µm Abundance (%)
Stations
72 71 70 69 68 67
40 35 30 25 20 15 10 5 0
27.25ºW
27.5ºW
27.75ºW
28ºW
Latitude

Figure 7.

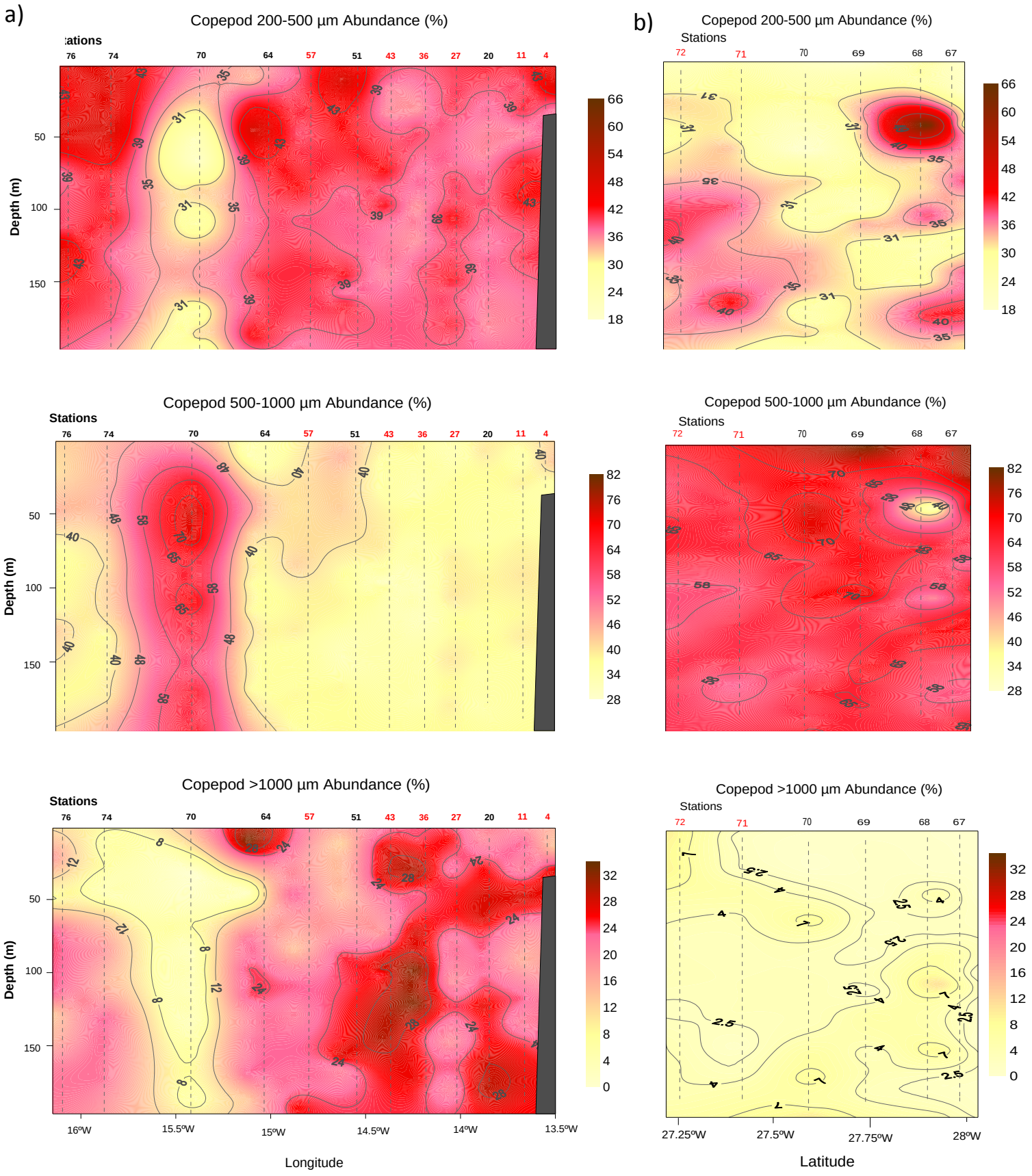
a)
Copepod 200-500 µm Abundance (%)
Stations
76 74 70 64 57 51 43 36 27 20 11 4
Depth (m)
50
100
150
66 60 54 48 42 36 30 24 18
b)
Copepod 200-500 µm Abundance (%)
Stations
72 71 70 69 68 67
66 60 54 48 42 36 30 24 18
Copepod 500-1000 µm Abundance (%)
Stations
76 74 70 64 57 51 43 36 27 20 11 4
Depth (m)
50
100
150
82 76 70 64 58 52 46 40 34 28
Copepod 500-1000 µm Abundance (%)
Stations
72 71 70 69 68 67
82 76 70 64 58 52 46 40 34 28
Copepod >1000 µm Abundance (%)
Stations
76 74 70 64 57 51 43 36 27 20 11 4
Depth (m)
50
100
150
32 28 24 20 16 12 8 4 0
16ºW 15.5ºW 15ºW 14.5ºW 14ºW 13.5ºW
Longitude
Copepod >1000 µm Abundance (%)
Stations
72 71 70 69 68 67
32 28 24 20 16 12 8 4 0
27.25ºW 27.5ºW 27.75ºW 28ºW
Latitude

Table 1. Regression and correlation parameters between body area and individual dry mass used for automated biomass calculations. SE, standard error of the regression coefficient *r*. Source: Lehette and Hernández-León (2009).

Taxonomical group	*a*	*b*±SE	*r*
Copepoda	43.97	1.52±0.02	0.972
Chaetognatha	23.45	1.19±0.13	0.840
Eupahusiid-like	49.58	1.48±0.05	0.987
Gelatinous	43.17	1.02±0.38	0.916
Other Mesozooplankton	43.38	1.54±0.03	0.947

Table 2. Mean (± SD) values of total species and copepod biomass (mg of dry weight · m^{-3}) in the two transects and the mesocale structures. The percentage of copepod biomass to the total biomass is also given.

	Transect 1	%	Transect 2	%	Upwelling	%	Filament	%	Anticyclonic eddy	%
Total	6.7±3.8		5.7±3.7		11.7±4.6		5.1±3.7		5.5±3.1	
Copepod	4.9±2.8	73.8	4.5±2.9	78.8	8.4±4.9	71.6	3.3±2.1	76.3	3.9±2.7	78.3

Table 3. Average (±SD) abundance (in %) of copepods and chaetognaths of the total value in the two transects and the mesoscale structures.

	Transect 1	Transect 2	Upwelling	Filament	Anticyclonic eddy
Copepod	82.4±9.5	94.8±2.4	83.2±7.3	84.4±7.7	82.9±12.1
Chaetognatha	9.5±6.8	3.7±1.4	5.5±3.1	10.3±6.9	11.3±7.1

Table 4. Average (±SD) abundance (in %) of the different size fractions for the total groups and copepods for the overall study region and the mesoscale structures.

	Total	Upwelling	Filament	Anticyclonic eddy
200-500 µm	28.2±9.1	21.1±6.3	31.7±10.5	30.9±9.5
500-1000 µm	61.1±9.1	65.7±5.6	52.4±10.3	63.2±7.9
>1000 µm	10.1±7.5	13.1±8.1	13.9±8.4	6.3±3.4
Copepod 200-500 µm	39.1±4.8	38.7±2.8	39.2±3.1	37.2±7.8
Copepod 500-1000 µm	40.9±8.8	37.2±2.1	36.7±3.6	49.6±12.9
Copepod >1000 µm	20.1±7.8	24.1±4.7	24.1±6.2	13.1±8.9